Article

Climate Change Impacts on Flow and Suspended Sediment Yield in Headwaters of High-Latitude Regions—A Case Study in China's Far Northeast

Yuyan Zhou [1,2] (ID)**, Y. Jun Xu [2,*]** (ID)**, Weihua Xiao [1,*], Jianhua Wang [1], Ya Huang [1,3] and Heng Yang [1]**

[1] State Key Laboratory of Simulation and Regulation of Water Cycle in River Basin, China Institute of Water Resources and Hydropower Research, Beijing 100038, China; zhouyuyan1@126.cm (Y.Z.); wjh@iwhr.com (J.W.); hygccw@163.com (Y.H.); yangheng890828@163.com (H.Y.)

[2] School of Renewable Natural Resources, Louisiana State University Agricultural Center, Baton Rouge, LA 70803, USA

[3] College of Civil Engineering and Architecture, Guangxi University, Nanning 530004, China

[*] Correspondence: yjxu@lsu.edu (Y.J.X.); xiaoweihua@iwhr.com (W.X.); Tel.: +1-225-578-4168 (Y.J.X.); +86-010-6878-1950 (W.X.)

Abstract: Climate change is expected to have stronger effects on water resources in higher latitude regions. Despite intensive research on possible hydrological responses in those regions to a warmer environment, our knowledge on erosion and sediment yield induced by the climate change in high-latitude headwaters is still limited. In this study, we estimated suspended sediment yields from 2021 to 2050 in a typical headwater area of far Northeast China to elucidate potential impacts of future climate change on surface runoff and erosion in higher latitude regions. We first parameterized the Soil and Water Assessment Tool (SWAT) using historical measurements to estimate runoff from the river basin. The model performed well in both the calibration (2006–2011) and the validation (2012–2014) periods, with an R^2 of 0.85 and 0.88 and a Nash-Sutcliffe Efficiency (NSE) of 0.7 and 0.73, respectively. We also utilized historical measurements on sediment yields from the period 2006–2014 to develop a runoff-sediment yield rating curve, and the rating curve obtained an excellent goodness of fit ($R^2 = 0.91$, $p < 0.001$). We then applied the calibrated SWAT model to two climate change projections, also known as Representative Concentration Pathways (RCP4.5 and RCP8.5), for the period from 2021 to 2050 to obtain future runoff estimates. These runoff estimates were then used to predict future sediment yield by using the developed runoff-sediment yield rating curve. Our study found a significant increase of annual sediment yield ($p < 0.05$) for both climate change projections (RCP4.5 = 237%; RCP8.5 = 133%) in this, China's high-latitude region. The increases of sediment yield were prevalent in summer and autumn, varying from 102–299% between the two RCPs scenarios. Precipitation was the dominated factor that determined the variation of runoff and sediment yield. A warming climate could bring more snowmelt-induced spring runoff and longer rainy days in autumn, hence leading to higher erosion. These findings demonstrate that under the changing climate, soils in this high-latitude headwater area would be eroded twice to three times that of the baseline period (1981–2010), indicating a potential risk to the downstream water quality and reservoir management.

Keywords: high-latitude regions; climate change; headwaters; sediment yield and erosion; Northeast China

1. Introduction

The relevance of climate change effects on the hydrological cycle in high-latitude river basins has been increasingly recognized in the recent decade [1–3]. These regions are of critical importance to mid-

and low latitudes in terms of changing climate, as the northern circumpolar region is a key driver of the global climate system [4]. High-latitude river basins are often snow—and/or glacial—dominated and will, hence, be more strongly affected by a warming climate [5,6]. Studies have demonstrated that global warming is intensifying hydrological cycles more in high-latitude regions than in other geographical regions, both temporarily and spatially [7,8].

Changes in surface runoff have been recognized by several recent studies as a direct response of high-latitude regions to a warming world. However, contradictory findings were reported from different regions. For instance, Li et al. reported a declining trend in annual discharge over the past six decades in the Songhua River Basin, one of the highest latitude river basins in China, due mainly to temperature [2]; Tape et al. found a decreasing trend of magnitude and frequency of runoff events in Arctic Alaska since 1980 [9]. However, in a modeling study, Donnelly et al. found a robust increase in runoff and discharge in the Scandinavian mountains over most of Norway, Sweden, and northern Poland [10]; Rood et al. reported a gradual increase of discharge from the Canadian largest river, the Mackenzie River, to the Arctic Ocean [11].

Headwaters are of great importance in river basin management because they have the longest cumulative length within a river basin [12,13]. They are also important in providing habitats and refuges for aquatic and riparian organisms, serving as both sink and source of sediment and nutrients, governing hydrologic connectivity and supplying and preserving clean water sources [14]. For instance, the headwaters of the Colorado River Basin generate about 75% of the annual streamflow from 25% of the area, while only 8% was contributed by the lower basin [15]. This makes these regions more vulnerable to global climate change in a river basin [16,17]. Jiang et al. examined the impacts of climate variability and anthropogenic activity on streamflow in the Three River Headwater region in China [18], which functions as the "water tower" of the East Asian river systems [19]. Javier et al. suggested that a 2 to 54% decrease of water resources was estimated in the headwaters of the Segura River Basin, which acts as the most important site of water resources generation in this river basin [20]. Though these findings have advanced the understandings of climate change impacts on headwater regions across various geographic locations, few studies have been conducted in headwaters in high-latitude regions. Even fewer have focused on the impacts on soil erosion and sediment yield in these regions.

Although it is reasonably believed in the research community that, where rainfall amounts in the future climate increase, surface erosion and sediment runoff will increase [21,22], effects of climate change on surface erosion and stream sediment yield in headwaters of world's cold regions are still uncertain. This is another important aspect for understanding future surface processes and stream, river, and lake water quality. Besides, higher temperature could lead to increasing snowmelt runoff and thus, potentially, increasing surface erosion [23]. A marked increase in suspended sediment concentration was observed in an Alpine catchment, owing to greater snowmelt caused by the rise in mean air temperature in the mid-1980s [24]. In a modeling study, Syvitski predicted that every 2 °C warming would lead to 22% increase in sediment flux carried by Arctic Rivers [25]. What is more, the impacts of changing precipitation on soil erosion can be combined with rising temperature. A warmer climate could raise the ratio of rainfall and snow, leading to more erosion, especially in spring and autumn times [26]. However, the contributions of temperature and precipitation to the fluctuations of sediment yield in high-latitude regions have not been fully understood due to scarce discharge and sediment observations in these regions.

The goal of this study aimed to determine the potential effects of future climate change on runoff, erosion, and riverine sediment in the headwaters of a China's high-latitude river basin, the Yinma River Basin (YRB). The YRB is located in China's far northeast and is a typical headwater region of the Songhua River Basin, one of the regions that are sensitive to climate change in China [26,27]. Although severe erosion has been reported in the Songhua River Basin [28], variations of soil erosion and sediment yield in headwaters have not been fully understood. As climate change persists, changes in surface runoff and streamflow in this cold region are expected. Hence, the study aimed to (1) assess the future trend of runoff and streamflow in the YRB under two climate change scenarios; (2) quantify

the impact of future climate change on erosion and stream sediment yield; and (3) determine major factors affecting temporal variation of runoff and sediment yield in the high-latitude region.

2. Materials and Methods

2.1. Study Area

This study selected the headwaters of the Yinma River Basin in Northeast China, which is a typical tributary basin to the Songhua River flowing northwards to the Amur River (Figure 1). This headwater region covers an area of 1861 km^2, with the elevation ranging from 188 to 1038 m a.m.s.l. The Changling stream gauging station (125°53′9.64″ E, 43°35′57.10″ N) is the headwater's outlet to the Shitoukoumen reservoir, which serves as a drinking water supply for Changchun, the Capitol of Jilin Province.
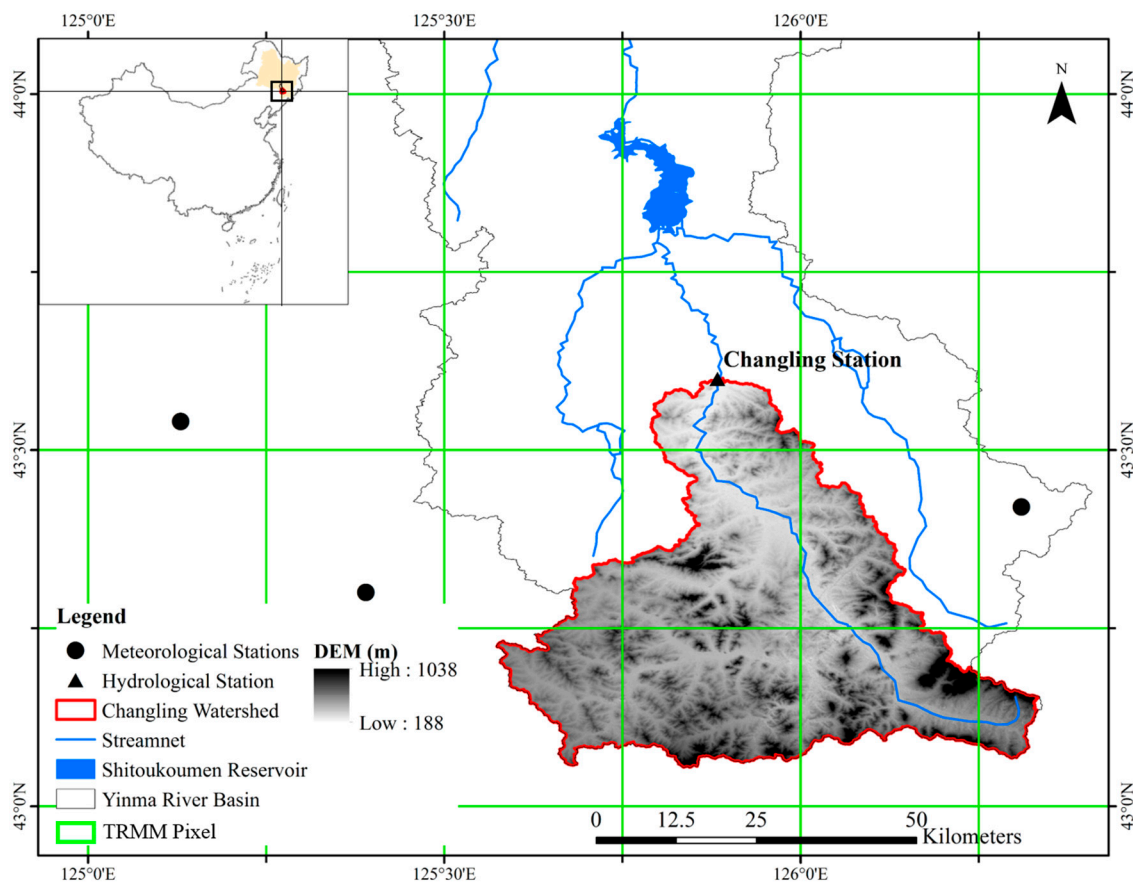

Figure 1. Changling watershed (1861 km^2), a headwater region of the Yinma River Basin (YRB) in Northeast China. Stream flow and sediment yields were measured at the Changling Station.

The area can be characterized by a typical cold temperate zone with continental monsoon climate, with a long-term annual mean temperature of 5.7 °C, varying from −15.7 °C in January to 22.9 °C in July, and a long-term annual mean precipitation of 654 mm, ranging from 422 to 1013 mm. The main land use of the study area is agricultural land, covering 49.8% of the area (Figure 2), followed by forested land. The main soil types in the headwater area are Cambisols and Phaeozems (FAO World Reference Base for Soil Resources), which cover nearly 50% of the total area (Figure 2).
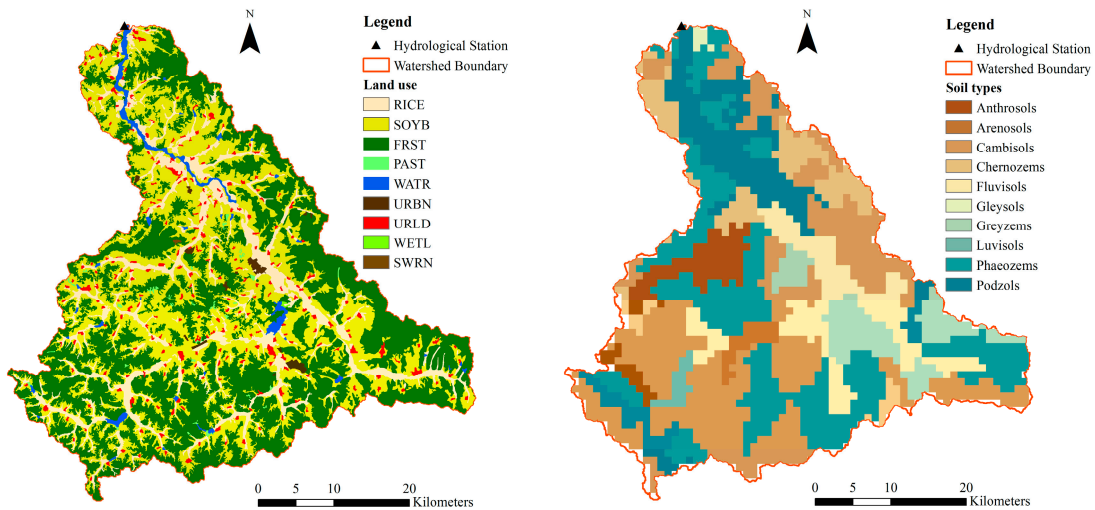
Figure 2. Land use/land cover (**left**) and soil types (**right**) of Changling watershed, the Yinma River headwater region in Northeast China.

2.2. Overall Study Design

This study employed a 4-step approach. First, we calibrated and validated the SWAT model and the parameterized model was used to represent existing conditions. Then, we applied the model with calibrated parameters to two climate change scenarios to obtain future surface runoff. Concurrently, we utilized historical streamflow and sediment yield records to develop a runoff-sediment yield rating curve. Finally, we used the simulated runoff and the rating to estimate future sediment yields. The approach is illustrated in Figure 3.
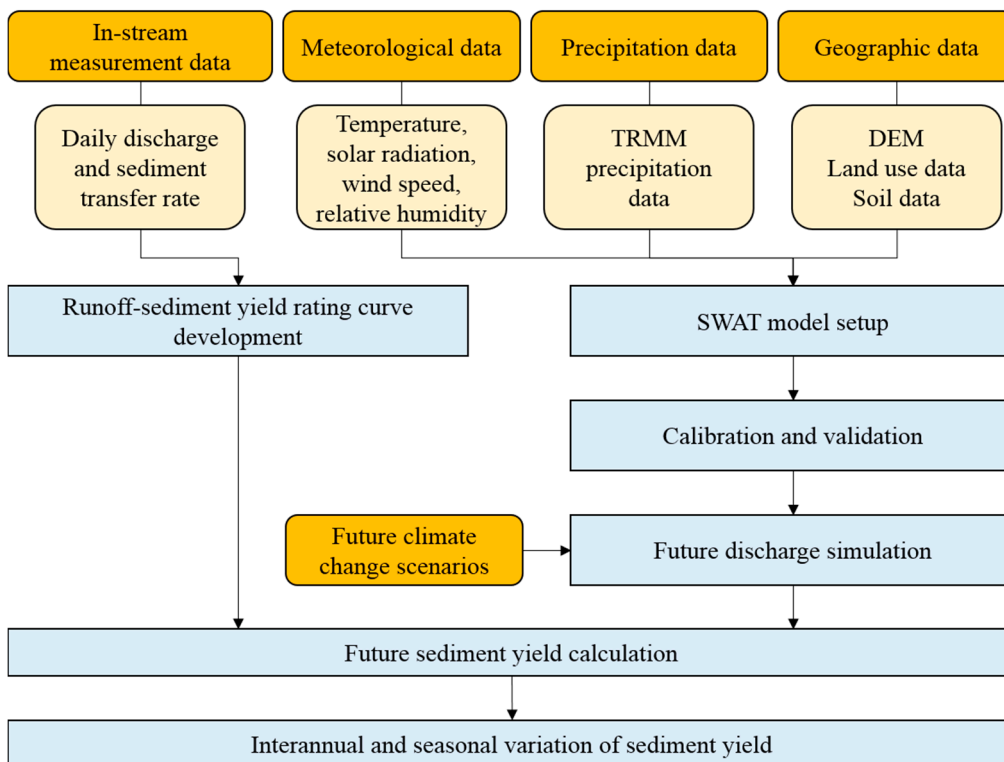

Figure 3. The overall research design and technical flowchart of this study.

2.3. Data Sources

Four types of data were used in this study including: (1) meteorological data; (2) satellite-based precipitation data; (3) river discharge and suspended sediment loads; and (4) spatially-referenced data, such as digital elevation model (DEM) data, land use/land cover data, and soil data. Daily average, maximum and minimum temperatures, relative humidity, solar radiation, and wind speed were obtained from China Meteorological Data Service Center (CMDC) for three meteorological stations around the headwater watershed (Figure 1) covering the period from 2006 to 2014.

Due to limitation of ground-based measurements on precipitation in this area, precipitation data were collected from the Tropic Rainfall Measuring Mission (TRMM) Multisatellite Precipitation Analysis (TMPA) [29]. In this study, we obtained 17 years of daily precipitation data of TRMM (3B42V7) at a resolution of $0.25° \times 0.25°$ (Figure 1). The meteorological data were used in the SWAT modeling to simulate monthly runoff from the headwater watershed.

River discharge (m^3/s) and suspended sediment loads (kg/s) were gathered from the Ministry of Water Resources of China for the Changling hydrological station covering the period from 2006 to 2014. Only suspended sediment particles were recorded at this hydrological station; therefore, suspended sediment yields were reported. The hydrology data were used to calibrate and validate the SWAT model, as well as develop a runoff– sediment load rating curve.

DEM data for the headwater area (Figure 1) were downloaded from the Integration and Training of National Agriculture Research Systems database, which has a spatial resolution of 90 m. The DEM was hydrologically corrected according to the actual channel network in the SWAT tool, and the actual channel network was obtained from the Channel Network Map provided by the Ministry of Water Resources of China. Land use data in 2005 with a spatial resolution of 1:100,000 used in this study was obtained from the Data Center for Resources and Environmental Sciences Chinese Academy of Sciences (RESDC). Soil type data were derived from the 1:1,000,000 soil map from the Institute of Soil Sciences Chinese Academy of Sciences. Details of the data sources were summarized in Table 1.

Table 1. Summary of data sources used in this study.

Data Type	Description	Data Sources
Meteorological data	Temperature, relative humidity, solar radiation, and wind speed	China Meteorological Data Service Center (CMDC, http://data.cma.cn/en)
Precipitation data	Daily TRMM precipitation data (3B42V7)	Tropic Rainfall Measuring Mission (TRMM) Multisatellite Precipitation Analysis (TMPA) (https://disc.gsfc.nasa.gov/datacollection/TRMM_3B42_Daily_7.html)
Hydrological and sedimentological data	Daily discharge and sediment transfer rate records	Hydrological data of Heilongjiang River Basin, Volume 2, Annual Hydrological Report of P.R. China, 2006–2014
Spatially-referenced data	Digital Elevation Model (DEM) (90 m × 90 m) Land use map in 2005 (1:100,000) Soil type (1:1,000,000)	Integration and Training of National Agriculture Research Systems database (http://srtm.csi.cgiar.org/). Data Center for Resources and Environmental Sciences Chinese Academy of Sciences (RESDC, http://www.resdc.cn). Institute of Soil Sciences Chinese Academy of Sciences (http://english.issas.cas.cn/).

2.4. SWAT Model Calibration and Validation

A spatially distributed hydrologic model, the Soil and Water Assessment Tool (SWAT), was applied for discharge and sediment yield estimation in this study. The inputs data for the SWAT model included precipitation, air temperature, solar radiation (SR), relative humidity (RH), and wind speed (WS). The model was first calibrated with discharge measurements made at the Changling Hydrological Station from 2006–2011, based on a configuration of 26 sub-basins as illustrated in Figure 4.
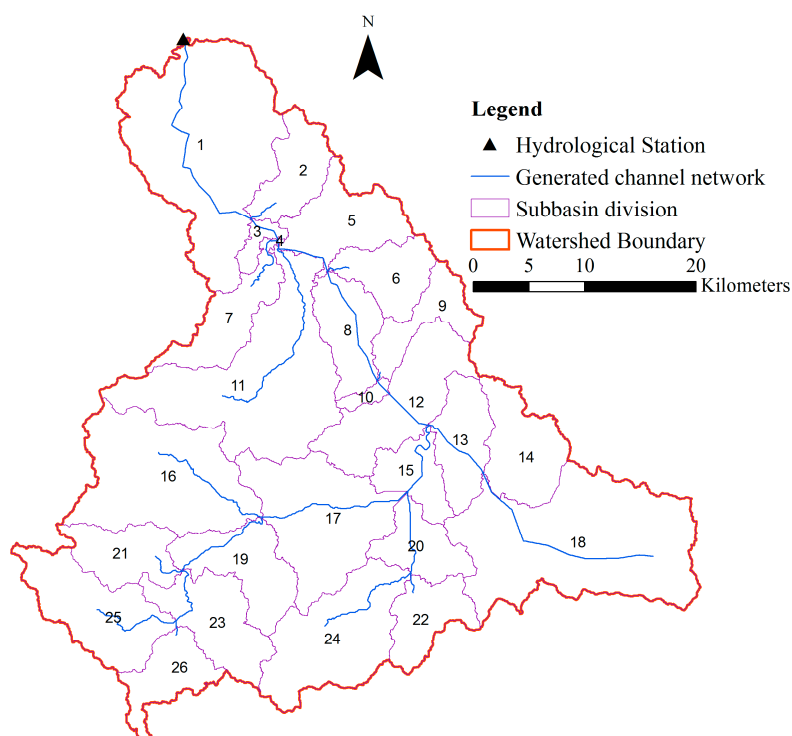
Figure 4. Configuration of the drainage network and sub-basins used for simulating discharge in the Yinma River headwater, Northeast China.

The calibrated model was then validated with discharge measurements from 2012–2014. Fitting values of sensitive model parameters calibrated are given in Table 2.

Table 2. Calibrated and validated model parameters used in Soil and Water Assessment Tool (SWAT).

Parameter	Description	Fitting Value
R__CN2.mgt	SCS runoff curve number for moisture condition II	−0.12
V__ALPHA_BF.gw	Base flow alpha factor	0.90
V__CH_K2.rte	Effective hydraulic conductivity in the main channel	54.94
V__CH_N2.rte	Manning's n value for main channel	0.27
V__SURLAG.bsn	Surface runoff lag time	3.79
R__SOL_AWC(..).sol	Soil available water storage capacity	1.07
R__SOL_K(..).sol	Soil conductivity	0.55
R__ESCO.hru	Soil evaporation compensation factor	0.93
V__GW_REVAP.gw	Groundwater revap. Coefficient	0.15
V__GWQMN.gw	Threshold depth of water in the shallow aquifer required for return flow to occur	2254.13
V__GW_DELAY.gw	Groundwater delay time	54.73
V__SFTMP.bsn	Snow fall temperature	−5.28
V__SMTMP.bsn	Snowfall melt base temperature	4.05
V__USLE_P.mgt	USLE equation support practice factor	0.36
V__USLE_K(..).sol	USLE equation parameter for soil erodibility	0.23
V__SPCON.bsn	Coefficient in sediment transport equation, linear parameter for calculating the maximum amount of sediment that can be re-entrained during channel sediment routing	0.0054
V__SPEXP.bsn	Exponent in sediment transport equation, exponent parameter for calculating sediment re-entrained in channel sediment routing	1.24
V__CH_COV1.rte	Channel erodibility factor	0.53
V__CH_COV2.rte	Channel cover factor	0.53

Both the calibration and validation for discharge simulation have obtained satisfactory goodness of fit with a coefficient of determination (R-squared, R^2) of 0.85 and 0.88 and a Nash–Sutcliffe efficiency (NSE) coefficient of 0.70 and 0.73, respectively (Table 3 and Figure 5). Results showed that the variation pattern of the simulated discharge was generally consistent with that of the observed discharge. For sediment yield simulation, the model performed well in simulating the fluctuation of the monthly sediment yield during 2006–2014. High R^2 for sediment yield simulation was found in both calibration and validation periods (0.72 and 0.74, respectively); however, relatively low NSEs were shown for the two periods (0.45 and 0.50, respectively) (Table 3 and Figure 5). In general, the hydrological model presented reasonable performances in simulating monthly discharge and sediment yield in the headwater watershed.

Table 3. Model performance statistics for discharge and sediment yield estimation, including Nash-Sutcliffe efficiency (NSE), coefficient of determination (R-squared), and percent bias (PBIAS).

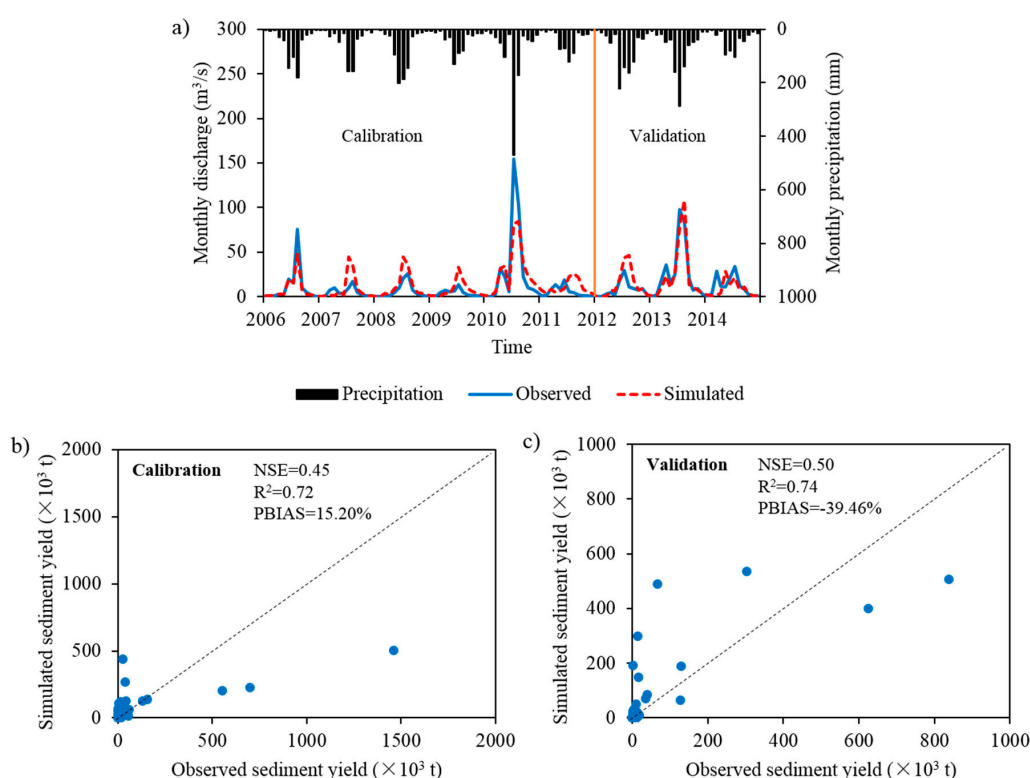| Simulation	Metrics	Calibration Period (2006–2011)	Validation Period (2012–2014)
Discharge simulation	NSE	0.7	0.73
	R-squared	0.85	0.88
	PBIAS (%)	−20.08	0.79
Sediment yield simulation	NSE	0.45	0.50
	R-squared	0.72	0.74
	PBIAS (%)	15.2	−39.46

Figure 5. (**a**) Model performance in discharge simulation during calibration and validation period, and model performances in sediment yield simulation during; (**b**) Calibration; (**c**) Validation period.

2.5. Runoff-Sediment Yield Rating Curve

The runoff-sediment yield rating curve was developed using the daily discharge and sediment yield data measured at the outlet of the headwater watershed (Changling Station, Figure 1). In high-latitude regions, soil erosion and sediment transportation were basically not triggered until

snowmelt and rainfall happened. Particularly, the suspended sediment load was largely transported in summer (especially July and August), with a highly simultaneous pattern with runoff and flood events [30]. Therefore, monthly runoff-sediment yield rating curve was constructed based on historical records during warm period. Warm period for a certain year is defined as those days that the average value of a continuous ten-day daily mean temperature is above the snowmelt temperature calibrated by the SWAT model, i.e., 4 degrees Celsius in this study (Table 2), both for historical period and future scenarios. Hence, monthly runoff-sediment yield rating curve for the headwater watershed is shown in Figure 6.
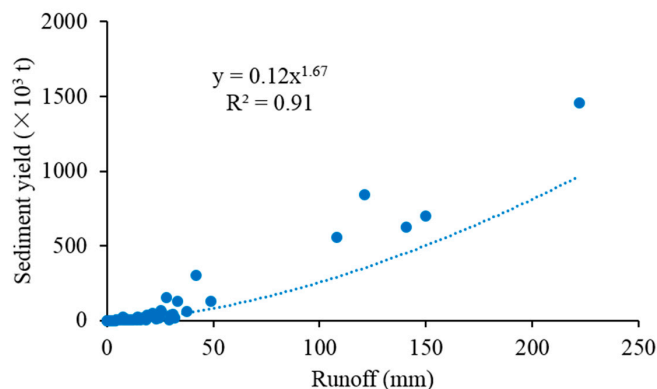

Figure 6. Numeric relationship ($p < 0.001$) between monthly runoff depth and sediment yield during the warm period.

2.6. Discharge and Sediment Yield Prediction

In this study, we only used the projected precipitation and minimum and maximum temperature downscaled at a high spatial resolution of 0.25° × 0.25° from the BNU-ESM model by the NASA Earth Exchange (NEX) Global Daily Downscaled Projections (GDDP) dataset (https://cds.nccs.nasa.gov/nex-gddp/) [31]. The future climate estimates in this dataset were provided at daily time scale, which makes them easy for SWAT model application. The downloaded climatic data were extracted for two periods, i.e., the baseline period (1981 to 2010) and the future period (2021 to 2050). Other climate factors, including solar radiation (SR), relative humidity (RH), wind speed (WS), and land use/land cover conditions were treated to be fixed for these two periods.

Two future climate scenarios, RCP4.5 and RCP8.5, were obtained from the downscaled, bias-corrected general circulation model (GCM), and the scenarios were based on two emission projections. Specifically, RCP4.5 represents a stabilization projection whereby total radiative forcing caused by greenhouse gas emissions is stabilized at 4.5 W·m^{-2} (approximately 650 ppm CO_2-equivalent) in the year 2100 without exceeding that value [32]; RCP8.5 is the worst case characterized by increasing greenhouse gas emissions over time, leading to high greenhouse gas concentration levels [33,34]. Statistical characteristics of precipitation and temperature for baseline and two future climate scenarios are summarized in Table 4.

The calibrated SWAT model was then employed to simulate discharge at Changling gauging station with downscaled climate data for the two periods. Afterwards, sediment yields during warm period were calculated using the predicted runoff and the established runoff-sediment yield rating curve. Sediment delivery ratio (SDR), defined as the ratio of sediment delivered at the catchment outlet to gross erosion within the basin [35], was calculated based on the results of the calibrated model. The SDR for this watershed ranges from 0.80 to 0.97, with an average value of 0.87 during 2006 to 2014, which indicates that 87% of the sediment exported from the headwaters of YRB was delivered to downstream. The SDR was set fixed during the baseline and predicted period. Soil erosion was then estimated by using sediment yield divided by the sediment delivery ratio.

Table 4. Precipitation and temperature for the baseline and two future climate change scenarios.

State Variables	Baseline	RCP4.5	RCP8.5
Mean annual precipitation (mm)	691	779	739
Mean annual rainfall (mm)	655	746	707
Mean annual rainy days	111	115	113
Mean annual rainfall intensity (mm/day)	5.9	6.5	6.2
Days of warm period	207	220	222
Mean annual mean temperature (°C)	5.3	7.5	8.0
Mean Annual minimum temperature (°C)	−29.3	−26.4	−26.6
Mean annual maximum temperature (°C)	33.5	34.8	35.2

Note: Precipitation falls as rain on those days when mean temperature is above snowfall temperature (i.e., −5.28 °C calibrated by the model). Rainy days are defined as those days with rainfall amount above 1mm. Rainfall intensity is the rainfall amount divided by the number of rainy days.

3. Results

3.1. Changes in Surface Runoff

Compared with the baseline period (1981–2010), we found that annual runoff in the headwaters of the Yinma River Basin would increase by 88% for RCP4.5 and by 48% for RCP8.5. The increases were statistically significant ($p < 0.05$, Table 5). Under the RCP4.5 conditions, the largest change in runoff was found in summer (130%), followed by that in autumn (57%) (Table 5). The runoff increase of these two seasons was statistically significant ($p < 0.05$, Table 5). Modeling results indicated that winter runoff would decrease by 39%, which was also statistically significant ($p < 0.05$, Table 5). For the RCP8.5 scenario, runoff of summer and autumn are expected to increase for 69% and 45%, respectively ($p < 0.05$, Table 5). However, spring and winter runoff showed a drop of 28% and 50% under RCP8.5, respectively, compared with baseline period (Table 5). Particularly, the falling of winter runoff for RCP8.5 was statistically significant ($p < 0.05$). By comparing the mean annual runoff for the two future scenarios, significantly less runoff was generated in the high-latitude headwaters under RCP8.5 than under RCP4.5 during the projected period ($p < 0.05$).

Table 5. Inter-annual variations of annual and seasonal precipitation, mean temperature, runoff, and sediment yield for the baseline period (1981–2010) and the predicted future (2021–2050) period under two climate change scenarios.

Scenarios	Precipitation		Mean Temperature		Runoff		Sediment Yield	
	Depth (mm)	Change (%)	(°C)	Change (%)	Depth (mm)	Change (%)	(×10³ t)	Change (%)
Baseline								
Annual	691	0	5.3	0	205	0	281	0
Spring	110	0	6.3	0	8	0	2	0
Summer	452	0	21.6	0	109	0	182	0
Autumn	129	0	6.7	0	75	0	96	0
Winter	1	0	−13.3	0	14	0	-	-
RCP4.5								
Annual	779	13% **	7.5	41% **	386	88% **	946	237% **
Spring	112	2%	8.9	40% **	11	35%	5	103%
Summer	538	19% **	23.5	9% **	249	130% **	727	299% **
Autumn	127	−1%	8.8	33% **	118	57% **	213	122% **
Winter	2	21%	−11.1	16% **	8	−39% **	-	-
RCP8.5								
Annual	739	7%	8.0	50% **	304	48% **	655	133% **
Spring	108	−1%	9.4	48% **	6	−28%	2	−37%
Summer	498	10% **	23.4	8% **	183	69% **	459	152% **
Autumn	132	3%	9.3	40% **	109	45% **	194	102% **
Winter	2	21%	−10.1	24% **	7	−50% **	-	-

Notes: * Significance at α = 0.05 level; ** Significance at α = 0.01 level.

On a monthly scale, runoff was expected to increase largely during summer and autumn months, while showing different variation patterns for RCP4.5 and RCP8.5 conditions. More runoff was expected to generate during summer and autumn times under RCP4.5 than that under RCP8.5. Spring runoff was estimated to increase under RCP4.5 condition, while dropping under RCP8.5. Runoff in winter times was expected to decrease for the two scenarios (Figure 7). The projected maximum runoff showed up in August for baseline and future period, reaching up to 52 mm (baseline), 126 mm (RCP4.5), and 103 mm (RCP8.5), leading to a maximum monthly runoff increase of 143% and 99%, respectively (Figure 7).
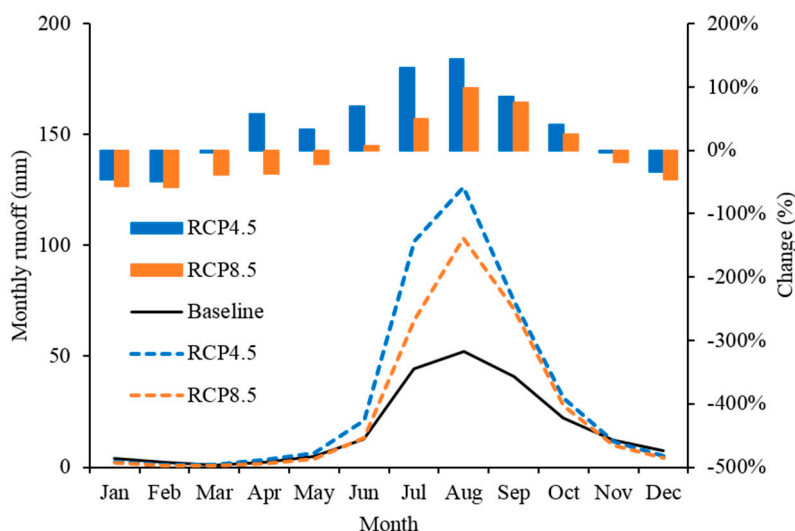

Figure 7. Monthly runoff variation for the baseline (1981–2010) and future (2021–2050) periods under two climate change scenarios.

3.2. Changes in Sediment Yield

The modeling results showed that annual sediment yields of the headwaters of the Yinma River Basin would increase by 237% under the RCP4.5 and by 133% under the RCP8.5 climate change projections ($p < 0.01$, Table 5). The increase of sediment yield would mainly occur in summer and autumn, ranging from 102% to 299%, which were statistically significant for both RCP scenarios ($p < 0.01$, Table 5). It should be noted that under RCP4.5, a 103% increase of sediment yield in the springs was estimated, while under RCP8.5 a 37% decrease of sediment yield in spring was expected.

The highest monthly sediment yields were found in August under both the baseline and future periods (Figure 8). The largest change in sediment yield by mass was also projected to occur in August under these two climate change scenarios. However, percentagewise, November would see the highest increase rate (718% for RCP4.5 and 666% for RCP8.5, Figure 8). These findings were consistent with the patterns shown in Table 5 that a significant increase was expected in summer and autumn. Besides, sediment yield under RCP4.5 was projected to increase in spring months, while SY under RCP8.5 showed a falling trend (Figure 8).
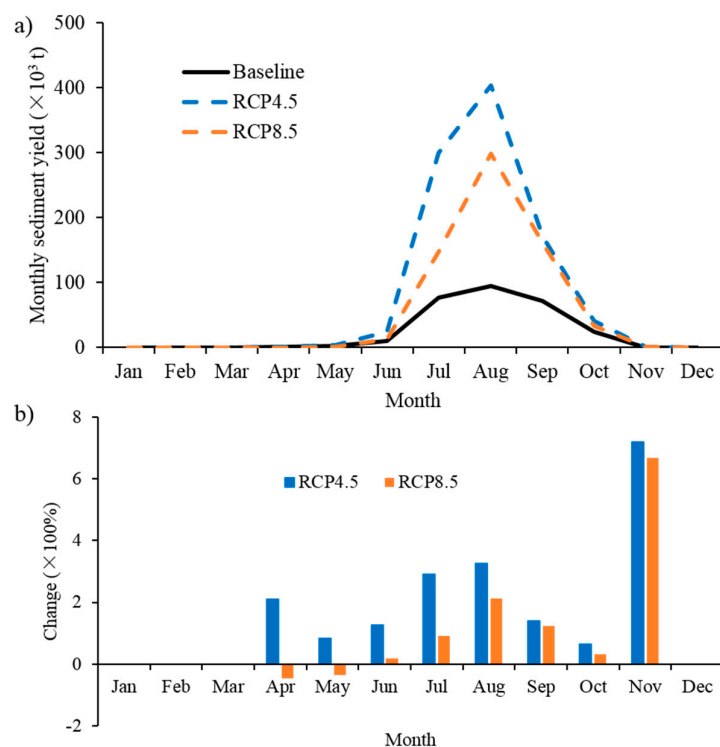
Figure 8. (**a**) Fluctuation of monthly sediment yields for the baseline (1981–2010) and future (2021–2050) periods. (**b**) Monthly changes of sediment yields between future and baseline period.

4. Discussion

4.1. Climate Change Impacts on Long-Term Runoff and Sediment Yield Trend

This modeling study demonstrates that both annual runoff and sediment yield in headwaters of a typical tributary basin of China's far northeast are expected to increase significantly in the future climate. This trend is similar to a recent modeling study by Li and Fang (2017) conducted in another headwater watershed in the region, though different modeling method and GCM scenarios were applied [28].

The most direct cause related to climate change for soil erosion variation is the changes in the erosive power of rainfall [36], i.e., rainfall erosivity. Though rainfall erosivity, also short for R-factor, was generally thought to be correlated to the product of total rainfall energy and maximum 30 min rainfall intensity during a storm [37], precipitation outputs from GCMs cannot provide precise information for R-factor calculation of each storm [22]. Therefore, statistical analysis on the relationships between annual precipitation and the R-factor was recommended to examine the future precipitation impacts on erosion and sediment yield [36]. Nearing et al. pointed out that rainfall amount and rainfall intensity were the two dominated factors accounting for the increase in precipitation, thus changing the rainfall erosivity [21,22].

In the high-latitude headwater watershed in this study, both annual rainfall amount and rainfall intensity were projected to increase under two future scenarios. Particularly, significant increases were found under RCP4.5 (Table 4). These could therefore lead to the rising of the R-factor in the headwater watershed. Statistical results also indicate that the variations of annual rainfall and rainfall intensity were more significant influencing factors than rainy days in determining the inter-annual changes of sediment yield of the headwater watershed (Table 6). Besides, no significant linear relationships were found between annual runoff/sediment yield and temperature. This indicates that though a warmer climate was projected in this study, the fluctuation of temperature did not account for the inter-annual variations of runoff and sediment yield.

Table 6. Pearson correlation coefficient between annual runoff/sediment and climatic factors under two climate change scenarios.

Scenarios	Variable	Precipitation (mm)	Rainfall (mm)	Rainfall Intensity (mm/Day)	Rainy Days
Baseline		0.81 **	0.82 **	0.80 **	0.29
RCP4.5	Annual runoff	0.92 **	0.92 **	0.89 **	0.42 *
RCP8.5		0.90 **	0.90 **	0.84 **	0.46 *
Baseline		0.81 **	0.82 **	0.81 **	0.27
RCP4.5	Annual sediment yield	0.89 **	0.90 **	0.87 **	0.39 *
RCP8.5		0.86 **	0.86 **	0.82 **	0.38 *

* Significance at α = 0.05 level; ** Significance at α = 0.01 level.

4.2. Climate Change Impacts on Seasonal Variation of Runoff and Sediment Yield

Our modeling results indicate that seasonal changes in precipitation and temperature could play an important role in future surface erosion and sediment yield. Significant increases in summer runoff and sediment yield in the high-latitude headwater watershed were found, accompanied by the rising of summer precipitation and temperature (Table 5). Similar results were also found in a recent study by Shrestha et al. [38] that stated that summer streamflow was expected to increase up to 63% under changing climate in the headwater region of the Athabasca River Basin, Canada. This may be mainly due to the fact that rainfall amounts in summer increase significantly for the two scenarios (Table 7). Particularly, more runoff and sediment yield in summer time were found under RCP4.5 than that under RCP8.5. This may be explained by the fact that summer rainfall, rainfall intensity, and rainy days under RCP4.5 were greater than that under RCP8.5 (Table 7), consequently leading to greater rainfall erosivity.

Table 7. Changes for annual and seasonal rainfall amount, rainfall intensity, and rainy days.

Rainfall Characteristics	Season	Value			Change (%)	
		Baseline	RCP4.5	RCP8.5	RCP4.5	RCP8.5
Rainfall Amount (mm)	Annual	655	746	707	14% **	8%
	Spring	98	101	97	4%	−1%
	Summer	442	529	489	20% **	11% *
	Autumn	116	115	121	0%	5%
Rainfall Intensity (mm/day)	Annual	5.9	6.5	6.2	9% *	5%
	Spring	4.1	4.3	4.4	5%	7%
	Summer	7.1	8.0	7.6	12% **	7%
	Autumn	4.5	4.4	4.5	−2%	−1%
Rainy Days	Annual	111	115	113	4%	2%
	Spring	24	23	22	−1%	−6%
	Summer	62	66	64	6% *	3%
	Autumn	25	25	27	2%	8%

Notes: * Significance at α = 0.05 level; ** Significance at α = 0.01 level.

Based on the simulation results, autumn runoff and sediment yield will likely increase significantly under both climate change scenarios, but the season's precipitation will not change (Table 5). For RCP4.5 condition, precipitation and rainfall amount is expected to decrease slightly, when compared with that in the baseline period. However, these two precipitation variables tend to increase slightly under RCP8.5 (Tables 5 and 7). Lower rainfall intensities is projected for the two future scenarios than in the baseline period, while more rainy days are expected (Table 7). This may be explained by the fact that warmer climate can raise the ratio of rainfall to snow by expanding the rainy days in autumn times (Table 7), which leads to the accumulation of sediment yield.

It should be noted that a 21% increase in winter precipitation but a 39% and a 50% decline in winter runoff were projected under RCP4.5 and RCP8.5, respectively. This may due to the fact that precipitation falls as snow during winter times, which would not trigger snowmelt runoff and rainfall-induced erosion until spring time. Therefore, less winter runoff was generated for the future period compared with baseline period.

Warming climate seemed to have a great impact in spring time as well. A 35% increase in spring runoff and a 103% increase in sediment yield under RCP4.5 may result from increasing snowmelt generated during warming springs (Table 5). The projected increases in discharge [17,38] and sediment yield [23,28] due to more snowmelt induced by warming spring have been reported in other high-latitude headwaters in the globe. However, decreasing in spring runoff and sediment yield under RCP8.5 was also projected, though a warmer condition was expected. This might be explained that precipitation plays a more dominant role in determining the variation of runoff and sediment yield, as explained above.

4.3. Uncertainties in Runoff and Sediment Yield Modeling

The results from this modeling study bear uncertainties. It is difficult to estimate individual contribution to the uncertainty of each source in evaluating the climate change impacts on runoff and sediment yield. Sources of the uncertainties may originate from the projected climate data by the general circulation models, the spatial hydrological modeling with SWAT, and the runoff-sediment rating curve method.

Improvements in increasing the precision and reducing the uncertainty of the hydrological model used to project the impacts of climate change on discharge and sediment yield are needed. Though a good agreement has been achieved in simulating the historical discharge of the headwater region, uncertainties in sediment yield modeling are still large. The soil loss simulation used in SWAT model was based on the Modified Universal Soil Loss Equations (MUSLE), developed by Williams [39]. However, this widely-used method is empirically-based. Recent progresses in developing models using physically-based equations to describe surface soil loss and sediment routing may improve sediment yield simulating results [28,40,41]. Besides, obtaining long-term hydrological measurements could help to refine the model evaluation processes.

Results also indicate that climate change impacts on sediment yield of these high-latitude headwaters are greater than on runoff due to the power function assumption of the rating curve [42–44]. The "black box" nature of this empirical method makes the sediment yield estimation site-specific and high-quality data-dependent, which brings greater uncertainties to the evaluation of the sensitivity of sediment yield to climate change [43]. However, this method could still be useful in revealing long-term sediment yield trend, especially in headwater regions where data are usually scarce. It is desirable to establish a better runoff-sediment yield relationship by obtaining long-term discharge and suspended sediment observations [44,45].

4.4. Environmental Implications

Mean annual soil erosion rates were 1.74, 5.84, and 4.04 $t \cdot ha^{-1} \cdot year^{-1}$ based on our calculation for the baseline period, RCP4.5 and RCP8.5 scenarios, respectively. This implies mean soil erosion rate of this high-latitude headwater watershed projected in historical times has exceeded the most commonly quoted tolerate soil loss rate (1 $t \cdot ha^{-1} \cdot year^{-1}$) [46–48]. The erosion rate of this headwater watershed was likely to continue increasing under future climate scenarios if no adaption strategies and measurements were undertaken. It has been estimated in this study that 87% of the eroded soil and sediment would be transported downstream of the river basin. This indicates that twice to three times the erosion from the headwater watershed would be delivered to lower stream regions by the middle of the 21st century.

Environmental and ecological risks of sediment-borne matters, e.g., particulate phosphorus, organic pollutants, or heavy metals, should be considered as well. A comprehensive water sampling

was conducted in the Yinma River Basin by Li et al. [49], in which high concentrations of heavy metals, i.e., Fe, Mn, and Hg, were found in summer and autumn. Sun et al. [50] reported that high environmental health risk of polycyclic aromatic hydrocarbons (PAHs) was found at the outlet of the headwater watershed. These pollutants, due to their low aqueous solubility and strong hydrophobic character, could be transported or deposited with sediment-associated phases [51,52], which may be a new but urgent warning to portable water supply and human health in the river basin given the projected rising of erosion and sediment yield. Studies conducted in forested headwaters also found that, when excess sediment reaches water bodies, organic matter or oxidizable inorganic nutrients could increase sediment oxygen demand (SOD) in the streambed [53–55], which could cause dissolved oxygen depletion [54,55] and stream metabolism [56].

Water resources and land management strategies that aim to prevent surface erosion due to changing climate, e.g., conservation tillage and vegetation cover maintaining, are therefore needed, especially for high flow periods in summer months and spring snowmelt periods. Measures that could efficiently cut down the sources of sediment-borne pollutants were also expected in this headwater watershed, e.g., eliminating excessive use of fertilization, reducing the risks of organic matters generated by wood and coal combustion, and erasing the accumulation of heavy metals in sediments caused by manufacturing and metallurgical industries spread in the river basin. Meanwhile, differences in climate change impacts between various emission scenarios (RCPs) should also be taken into account when formulating these strategies.

5. Conclusions

This study investigated climate change impacts on surface runoff and sediment yield in a high-latitude headwater region of China. Changes in runoff and sediment yield of the headwaters under two future climate scenarios, a stabilization projection (RCP4.5) and a projection without stabilization (RCP8.5), were evaluated using a combined approach of a calibrated hydrological model and a runoff-sediment yield rating curve. The modeling results show that both climate change projections for 2021–2050 would increase annual surface runoff and sediment yield compared with the baseline period (1981–2010). Sediment yield would increase by 237% for RCP4.5 and 133% for RCP8.5, primarily caused by precipitation changes. The increase seemed to be prevalent in summer and autumn, varying from 102 to 299% between the two RCPs scenarios. A warming climate could bring more snowmelt-induced spring runoff and longer rainy days in autumn, altering the spring and autumn sediment yield. This study indicates that increases in runoff and sediment yield will likely occur in the world's high-latitude headwaters under a changing climate, both at the yearly and seasonal scales, which needs to be considered in future water resources management and land use management at the river basin scale. The framework and findings of this study are widely applicable to other high-latitude headwater regions, especially those that are data-scarce.

Author Contributions: Yuyan Zhou carried out the study, analyzed the data, and wrote the first manuscript draft. Y. Jun Xu and Weihua Xiao developed the study concept, provided oversight throughout the study, and revised the manuscript. Jianhua Wang provided valuable comments in revising the manuscript. Ya Huang and Heng Yang assisted in dealing with the meteorological data analysis.

Conflicts of Interest: The authors declare no conflict of interest.

References

1.　Meng, D.; Mo, X. Assessing the effect of climate change on mean annual runoff in the songhua river basin, China. *Hydrol. Process.* **2012**, *26*, 1050–1061. [CrossRef]

2.   Li, F.; Zhang, G.; Xu, Y.J. Spatiotemporal variability of climate and streamflow in the Songhua river basin, northeast China. *J. Hydrol.* **2014**, *514*, 53–64. [CrossRef]

3.   Barnett, T.P.; Adam, J.C.; Lettenmaier, D.P. Potential impacts of a warming climate on water availability in snow-dominated regions. *Nature* **2005**, *438*, 303–309. [CrossRef] [PubMed]

4.   Francis, J.A.; White, D.M.; Cassano, J.J.; Gutowski, W.J.; Hinzman, L.D.; Holland, M.M.; Steele, M.A.; Vörösmarty, C.J. An arctic hydrologic system in transition: Feedbacks and impacts on terrestrial, marine, and human life. *J. Geophys. Res.* **2009**, *114*. [CrossRef]

5.   Laudon, H.; Spence, C.; Buttle, J.; Carey, S.K.; McDonnell, J.J.; McNamara, J.P.; Soulsby, C.; Tetzlaff, D. Save northern high-latitude catchments. *Nat. Geosci.* **2017**, *10*, 324–325. [CrossRef]

6.   Moore, G.W. The december 2015 north pole warming event and the increasing occurrence of such events. *Sci. Rep.* **2016**, *6*, 39084. [CrossRef] [PubMed]

7.   Serreze, M.C.; Francis, J.A. The arctic amplification debate. *Clim. Chang.* **2006**, *76*, 241–264. [CrossRef]

8.   Nijssen, B.; O'Donnell, G.M.; Hamlet, A.F.; Lettenmaier, D.P. Hydrologic vulnerability of global rivers to climate change. *Clim. Chang.* **2001**, *50*, 143–175. [CrossRef]

9.   Tape, K.D.; Verbyla, D.; Welker, J.M. Twentieth century erosion in arctic alaska foothills: The influence of shrubs, runoff, and permafrost. *J. Geophys. Res.* **2011**, *116*. [CrossRef]

10.   Donnelly, C.; Greuell, W.; Andersson, J.; Gerten, D.; Pisacane, G.; Roudier, P.; Ludwig, F. Impacts of climate change on european hydrology at 1.5, 2 and 3 degrees mean global warming above preindustrial level. *Clim. Chang.* **2017**, *143*, 13–26. [CrossRef]

11.   Rood, S.B.; Kaluthota, S.; Philipsen, L.J.; Rood, N.J.; Zanewich, K.P. Increasing discharge from the mackenzie river system to the arctic ocean. *Hydrol. Process.* **2017**, *31*, 150–160. [CrossRef]

12.   Benda, L.; Hassan, M.A.; Church, M.; May, C.L. Geomorphology of steepland headwaters: The transition from hillslopes to channels. *J. Am. Water Resour. Assoc.* **2005**, *41*, 835–851. [CrossRef]

13.   Freeman, M.C.; Pringle, C.M.; Jackson, C.R. Hydrologic connectivity and the contribution of stream headwaters to ecological integrity at regional scales. *J. Am. Water Resour. Assoc.* **2007**, *43*, 5–14. [CrossRef]

14.   Wohl, E. The significance of small streams. *Front. Earth Sci.* **2017**, *11*, 447–456. [CrossRef]

15.   Gao, Y.; Vano, J.A.; Zhu, C.; Lettenmaier, D.P. Evaluating climate change over the colorado river basin using regional climate models. *J. Geophys. Res.* **2011**, *116*. [CrossRef]

16.   Bales, R.C.; Molotch, N.P.; Painter, T.H.; Dettinger, M.D.; Rice, R.; Dozier, J. Mountain hydrology of the western united states. *Water Resour. Res.* **2006**, *42*, W08432. [CrossRef]

17.   Zhang, A.; Liu, W.; Yin, Z.; Fu, G.; Zheng, C. How will climate change affect the water availability in the heihe river basin, northwest China? *J. Hydrometeorol.* **2016**, *17*, 1517–1542. [CrossRef]

18.   Jiang, C.; Li, D.; Gao, Y.; Liu, W.; Zhang, L. Impact of climate variability and anthropogenic activity on streamflow in the three rivers headwater region, Tibetan plateau, China. *Theor. Appl. Climatol.* **2016**, *129*, 667–681. [CrossRef]

19.   Fang, Y. Managing the three-rivers headwater region, china: From ecological engineering to social engineering. *Ambio* **2013**, *42*, 566–576. [CrossRef] [PubMed]

20.   Senent-Aparicio, J.; Pérez-Sánchez, J.; Carrillo-García, J.; Soto, J. Using SWAT and fuzzy topsis to assess the impact of climate change in the headwaters of the segura river basin (SE Spain). *Water* **2017**, *9*, 149. [CrossRef]

21.   Pruski, F.F.; Nearing, M.A. Runoff and soil-loss responses to changes in precipitation: A computer simulation study. *J. Soil Water Conserv.* **2002**, *57*, 7–16.

22.   Nearing, M.A.; Pruski, F.F.; O'Neal, M.R. Expected climate change impacts on soil erosion rates: A review. *J. Soil Water Conserv.* **2004**, *59*, 43–50.

23.   Asselman, N.E.M.; Middelkoop, H.; van Dijk, P.M. The impact of changes in climate and land use on soil erosion, transport and deposition of suspended sediment in the river Rhine. *Hydrol. Process.* **2003**, *17*, 3225–3244. [CrossRef]

24.   Costa, A.; Molnar, P.; Stutenbecker, L.; Bakker, M.; Silva, T.A.; Schlunegger, F.; Lane, S.N.; Loizeau, J.-L.; Girardclos, S. Temperature signal in suspended sediment export from an alpine catchment. *Hydrol. Earth Syst. Sci. Discuss.* **2017**, 1–30. [CrossRef]

25.   Syvitski, J.P.M. Sediment discharge variability in arctic rivers: Implications for a warmer future. *Pol. Res.* **2002**, *21*, 323–330. [CrossRef]

26. Zhang, Y.G.; Nearing, M.A.; Zhang, X.C.; Xie, Y.; Wei, H. Projected rainfall erosivity changes under climate change from multimodel and multiscenario projections in northeast China. *J. Hydrol.* **2010**, *384*, 97–106. [CrossRef]

27. Wei, Z.; Jin, H.; Zhang, J.; Yu, S.; Han, X.; Ji, Y.; He, R.; Chang, X. Prediction of permafrost changes in northeastern china under a changing climate. *Sci. China Earth Sci.* **2011**, *54*, 924–935. [CrossRef]

28. Li, Z.; Fang, H. Modeling the impact of climate change on watershed discharge and sediment yield in the black soil region, northeastern China. *Geomorphology* **2017**, *293*, 255–271. [CrossRef]

29. Huffman, G.J.; Bolvin, D.T.; Nelkin, E.J.; Wolff, D.B.; Adler, R.F.; Gu, G.; Hong, Y.; Bowman, K.P.; Stocker, E.F. The trmm multisatellite precipitation analysis (TMPA): Quasi-global, multiyear, combined-sensor precipitation estimates at fine scales. *J. Hydrometeorol.* **2007**, *8*, 38–55. [CrossRef]

30. Nu-Fang, F.; Zhi-Hua, S.; Lu, L.; Cheng, J. Rainfall, runoff, and suspended sediment delivery relationships in a small agricultural watershed of the Three Gorges area, China. *Geomorphology* **2011**, *135*, 158–166. [CrossRef]

31. Thrasher, B.; Maurer, E.P.; McKellar, C.; Duffy, P.B. Technical note: Bias correcting climate model simulated daily temperature extremes with quantile mapping. *Hydrol. Earth Syst. Sci.* **2012**, *16*, 3309–3314. [CrossRef]

32. Thomson, A.M.; Calvin, K.V.; Smith, S.J.; Kyle, G.P.; Volke, A.; Patel, P.; Delgado-Arias, S.; Bond-Lamberty, B.; Wise, M.A.; Clarke, L.E.; et al. Rcp4.5: A pathway for stabilization of radiative forcing by 2100. *Clim. Chang.* **2011**, *109*, 77–94. [CrossRef]

33. Riahi, K.; Grübler, A.; Nakicenovic, N. Scenarios of long-term socio-economic and environmental development under climate stabilization. *Technol. Forecast. Soc. Chang.* **2007**, *74*, 887–935. [CrossRef]

34. Riahi, K.; Rao, S.; Krey, V.; Cho, C.; Chirkov, V.; Fischer, G.; Kindermann, G.; Nakicenovic, N.; Rafaj, P. Rcp 8.5—A scenario of comparatively high greenhouse gas emissions. *Clim. Chang.* **2011**, *109*, 33–57. [CrossRef]

35. Walling, D.E. The sediment delivery problem. *J. Hydrol.* **1983**, *65*, 209–237. [CrossRef]

36. Nearing, M.A. Potential changes in rainfall erosivity in the U.S. With climate change during the 21st century. *J. Soil Water Conserv.* **2001**, *56*, 229–232.

37. Wischmeier, W.H.; Smith, D.D. Predicting Rainfall-Erosion Losses from Cropland East of the Rocky Mountains: Guide for Selection of Practices for Soil and Water Conservation. Agricultural Research Service, U.S. Dept of Agriculture in cooperation with Purdue Agricultural Experiment Station, 1965. Available online: https://naldc.nal.usda.gov/download/CAT87208342/PDF (accessed on 7 December 2017).

38. Shrestha, N.K.; Du, X.; Wang, J. Assessing climate change impacts on fresh water resources of the athabasca river basin, Canada. *Sci. Total Environ.* **2017**, *601–602*, 425–440. [CrossRef] [PubMed]

39. Williams, J.R. Sediment routing for agricultural watersheds. *Water Resour. Bull.* **1975**, *11*, 965–974. [CrossRef]

40. Bussi, G.; Francés, F.; Horel, E.; López-Tarazón, J.A.; Batalla, R.J. Modelling the impact of climate change on sediment yield in a highly erodible mediterranean catchment. *J. Soils Sediments* **2014**, *14*, 1921–1937. [CrossRef]

41. Buendia, C.; Bussi, G.; Tuset, J.; Vericat, D.; Sabater, S.; Palau, A.; Batalla, R.J. Effects of afforestation on runoff and sediment load in an upland mediterranean catchment. *Sci. Total Environ.* **2016**, *540*, 144–157. [CrossRef] [PubMed]

42. Walling, D.E. Suspended sediment production and building activity in a small british basin. *IAHS Publ.* **1974**, *113*, 137–144. Available online: http://hydrologie.org/redbooks/a113/iahs_113_0137.pdf (accessed on 7 December 2017).

43. Asselman, N.E.M. Fitting and interpretation of sediment rating curves. *J. Hydrol.* **2000**, *234*, 228–248. [CrossRef]

44. Crawford, C.G. Estimation of suspended-sediment rating curves and mean suspended-sediment loads. *J. Hydrol.* **1991**, *129*, 331–348. [CrossRef]

45. Horowitz, A.J. An evaluation of sediment rating curves for estimating suspended sediment concentrations for subsequent flux calculations. *Hydrol. Process.* **2003**, *17*, 3387–3409. [CrossRef]

46. Li, Z.; Fang, H. Impacts of climate change on water erosion: A review. *Earth-Sci. Rev.* **2016**, *163*, 94–117. [CrossRef]

47. Jones, R.J.; Le Bissonnais, Y.; Bazzoffi, P.; Sanchez Diaz, J.; Düwel, O.; Loj, G.; Øygarden, L.; Prasuhn, V.; Rydell, B.; Strauss, P. Nature and Extent of Soil Erosion in Europe. 2004. Available online: http://eusoils.jrc.ec.europa.eu/ESDB_Archive/pesera/pesera_cd/sect_h1.htm (accessed on 7 December 2017).

48. Verheijen, F.G.A.; Jones, R.J.A.; Rickson, R.J.; Smith, C.J. Tolerable versus actual soil erosion rates in Europe. *Earth-Sci. Rev.* **2009**, *94*, 23–38. [CrossRef]

49. Li, S.; Zhang, J.; Mu, G.; Ju, H.; Wang, R.; Li, D.; Shabbir, A. Spatiotemporal characterization of chromophoric dissolved organic matter (CDOM) and CDOM-DOC relationships for highly polluted rivers. *Water* **2016**, *8*, 399. [CrossRef]

50. Sun, C.; Zhang, J.; Ma, Q.; Chen, Y.; Ju, H. Polycyclic aromatic hydrocarbons (PAHs) in water and sediment from a river basin: Sediment-water partitioning, source identification and environmental health risk assessment. *Environ. Geochem. Health* **2017**, *39*, 63–74. [CrossRef] [PubMed]

51. Tolosa, I.; de Mora, S.; Sheikholeslami, M.R.; Villeneuve, J.-P.; Bartocci, J.; Cattini, C. Aliphatic and aromatic hydrocarbons in coastal caspian sea sediments. *Mar. Pollut. Bull.* **2004**, *48*, 44–60. [CrossRef]

52. Cardellicchio, N.; Buccolieri, A.; Giandomenico, S.; Lopez, L.; Pizzulli, F.; Spada, L. Organic pollutants (PAHs, PCBs) in sediments from the mar piccolo in taranto (Ionian Sea, Southern Italy). *Mar. Pollut. Bull.* **2007**, *55*, 451–458. [CrossRef] [PubMed]

53. Matlock, M.D.; Kasprzak, K.R.; Osborn, G.S. Sediment oxygen demand in the arroyo Colorado River. *J. Am. Water Resour. Assoc.* **2003**, *39*, 267–275.

54. Jason Todd, M.; Vellidis, G.; Richard Lowrance, R.; Pringle, C.M. High sediment oxygen demand within an instream swamp in southern georgia: Implications for low dissolved oxygen levels in coastal blackwater streams. *J. Am. Water Resour. Ass.* **2009**, *45*, 1493–1507. [CrossRef]

55. DaSilva, A.; Xu, Y.J.; Beebe, J.; Ice, G.G. Effects of timber harvesting on dissolved oxygen in a Northern Louisiana headwater stream. *For. Sci.* **2013**, *59*, 127–138. [CrossRef]

56. DaSilva, A.; Xu, Y.; Ice, G.; Beebe, J.; Stich, R. Effects of timber harvesting with best management practices on ecosystem metabolism of a low gradient stream on the united states gulf coastal plain. *Water* **2013**, *5*, 747–766. [CrossRef]